Solar coronal loops and remarks

Linda Sugiyama

CEMM meeting, Sherwood 2016

April 3, 2016

Topics

- MHD model for solar coronal loops, based on magnetic torus*
  - Nonaxisymmetric steady state with gravity
- Remarks on comparison of M3D-C1 and M3D for edge instability

*Submitted to PRL (2016); expanded version in progress.

Solar coronal loops

- Solar coronal loop as a magnetic flux rope
- FIRST and only MHD steady state model (analytic)
  - Full force balance in toroidal, non-axisymmetric geometry
  - Radial expansion instability (major radius) of a curved toroidal system is stabilized by the non-axisymmetric solar gravity
  - Parameter $\hat{G} = ga/v_A^2$, g=acceleration due to gravity
- Only two solutions exist at high beta ($\beta \sim \varepsilon^1$), $\hat{G} \sim \varepsilon^3$ and $\hat{G} \sim \varepsilon^2$ for inverse aspect ratio $\varepsilon = a/R_o \sim 0.02$
  - Loop height and non-axisymmetry scale with $\hat{G}$
  - Solutions can be related to high beta tokamak, stellarator
- Good fit to observed loops!!
- Implications for solar physics, non-axisymmetric tori

Magnetic flux ropes

- A variety of solar loops exist: Consider coronal loops in solar active regions that connect photospheric magnetic flux regions of opposite polarity, with loop heights < R_{sun}
- Generally accepted that coronal loops are magnetic flux ropes that contain plasma. Lower ends are connected to the photosphere, where their structure is unknown
- Temperature and density are higher than in the surrounding solar corona
  - Visible bright emission curve observed in spectral lines
  - A major question for loop physics is to explain high T
- Quasi-steady state – typical lifetimes of minutes to hours (1000-5000 s for warm loops at T=1-3 MK)

Coronal loops in a solar active region

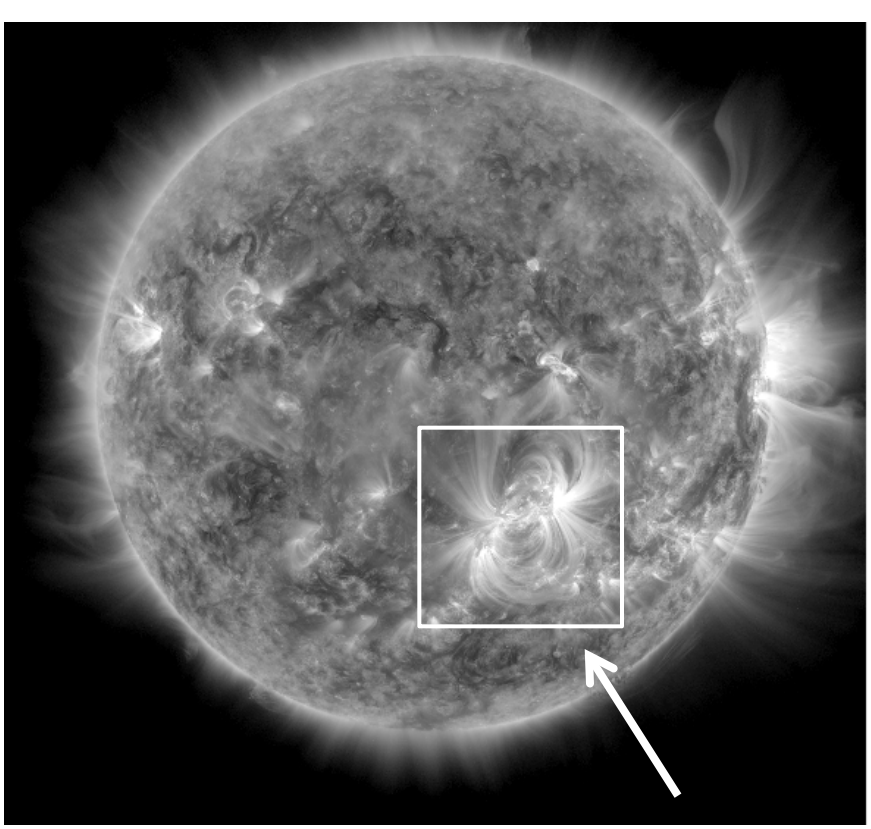

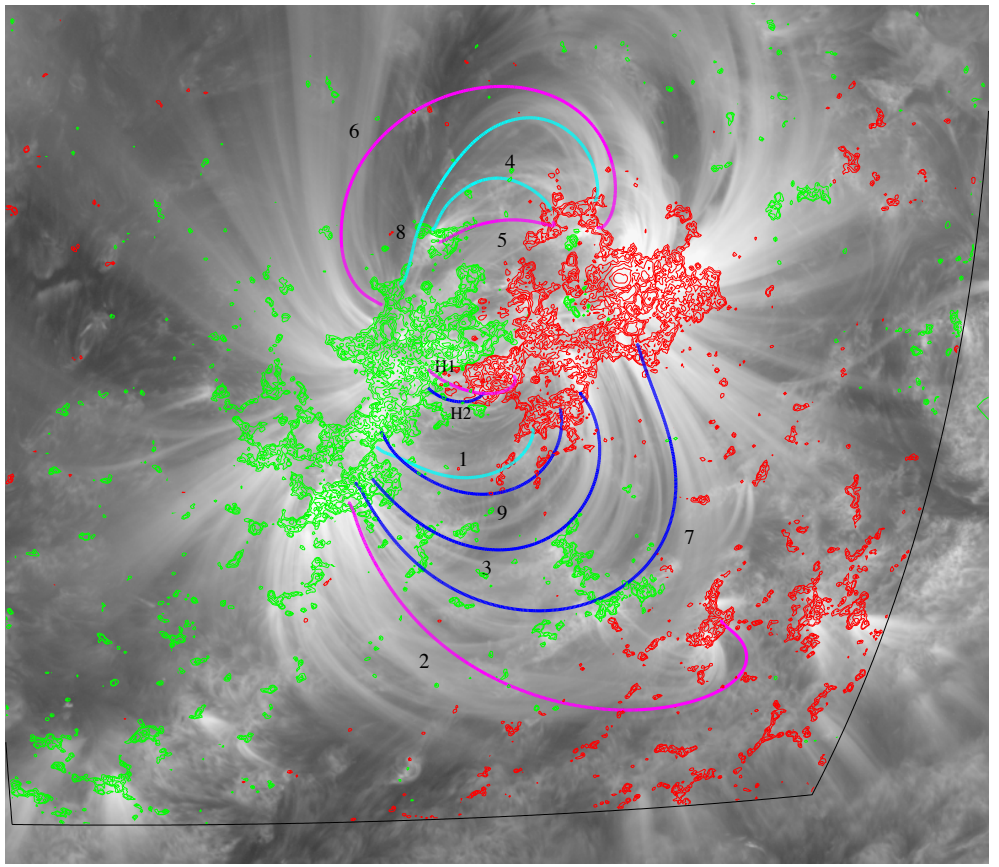

- Solar active region NOAA 11564 on Sep 7, 2012
- Background: emission at 171 Å from AIA on the Solar Data Observatory (SDO)
- Magnetic field lines, from NLFF magnetic model, match bright emission curves. Red (+) and green (-) show photospheric magnetic flux polarity ($B_n \gtrless 0$)
- Warm (T=1-3MK) or short hot (`H', T$\gtrsim$5 MK) loops – shown in Table I

What's new?

- No steady state model for coronal loop structure exists!
  MHD steady states not previously considered, due to difficulty of solar observations.
- Solar observations must be interpreted using models
  - Hydrostatic pressure, density in corona: $\nabla p + \rho g \mathbf{h}=0$ for solar vertical **h** gives $\rho=\rho_o \exp(- gh/(T/M))$ for a constant temperature T
  - Nonlinear force-free field (NLFF) model for **B**: $\mathbf{J}\times\mathbf{B}=0$, $\mathbf{B}=\nabla\Phi$
- No observations exist at the required level of detail
  - No loop cross section or boundary shapes, pressure/temperature/ density profiles, ∇p (still true)
  - ``Small'' gravity ignored, except a few loop heating models
  - Radial expansion instability for large loops, in coronal mass ejections
- Construction of loop steady states requires knowledge of MHD toroidal equilibria – known from magnetic fusion!

Toroidal magnetic flux rope model

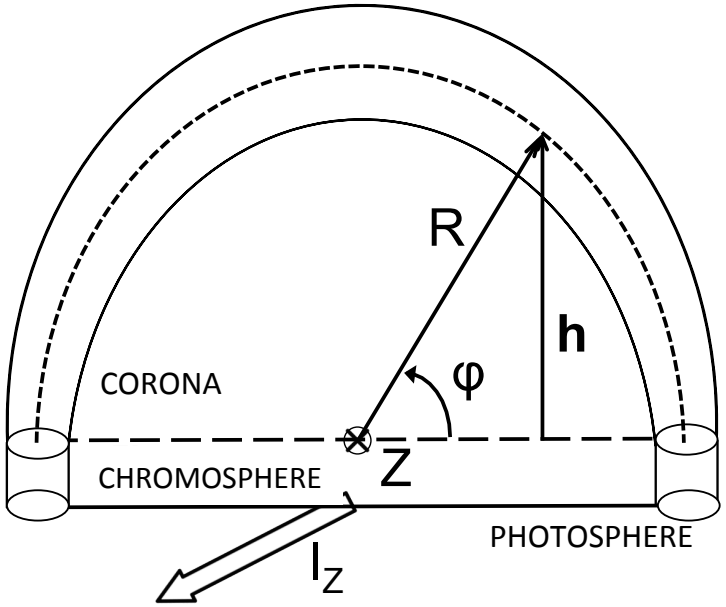

Coronal loop

Cylindrical coordinates (R,Z,ϕ)
Solar vertical height **h**
Solar regions:
Photosphere|chromosphere|corona
Model considers only coronal part

- Loop is half of a magnetic torus; field lines are tied to structures in the photosphere and below (model valid for general sector)
- Assume that the toroidal field has form $B_\phi=(R_oB_o/R)(1+\varepsilon\tilde{I})$, i.e., generated by an ``axial current'' I_Z
- Assume gravity is the only source of non-axisymmetry

  Force $-\rho g\hat{\mathbf{h}}$, $\hat{\mathbf{h}} = \hat{\mathbf{R}}\cos\phi + \boldsymbol{\phi}\sin\phi$, acceleration g=274.93 m/s^2

Evidence for ``axial current''

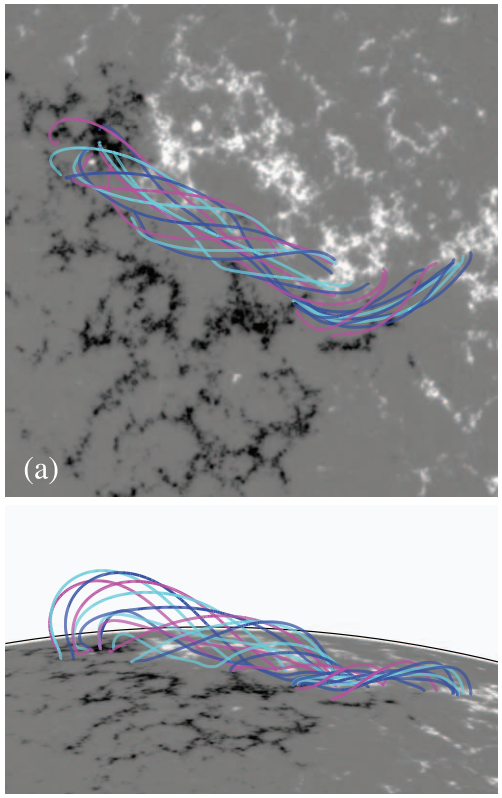

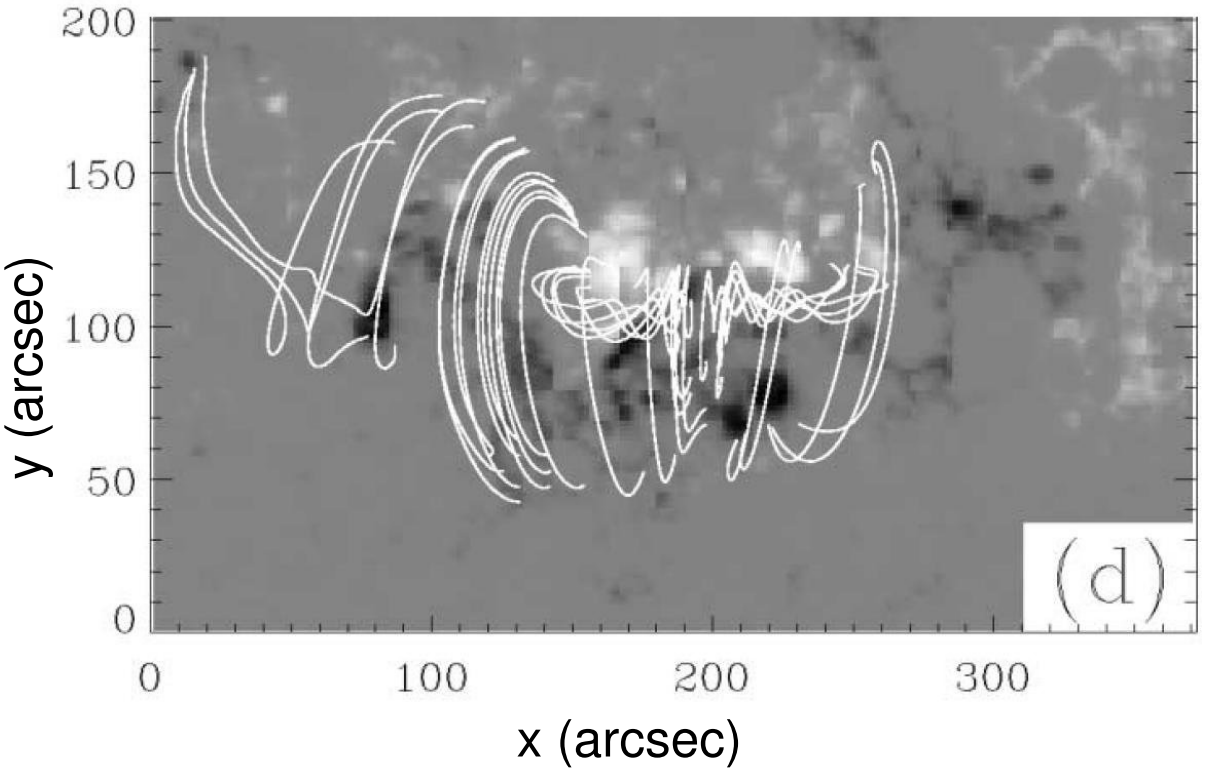

- Rarely, a wide, thin, low altitude, current-carrying ``flux rope'' is seen in the corona, aligned parallel to the opposite-polarity magnetic flux regions.
- Higher coronal loops arch across it, connecting the two flux regions

  (Left: Bobra et al., Ap. J. (2008). Right: Yan et al., Ap. .J (2001), with higher loops.)
- Such large, low flux ropes may initiate one type of Coronal Mass Ejection. (Not described by present model)

Radial expansion instability of curved loop

- Toroidal current-carrying magnetic loops are unstable to radial expansion (major radius) driven by the force imbalance between the inside and outside of the torus, due to its curvature
  - (1/R) due to B_ϕ (Force $F_R \sim p\,\mathcal{A}\Delta\phi$ integrated over a toroidal sector $R\Delta\phi$)
  - ∇p (Force $F_p \sim p\,\mathcal{A}\Delta\phi$; $\mathcal{A}$=area$_\perp$)
  - Hoop force due to B_{pol} generated by loop current I_ϕ (Force $F_H \sim \varepsilon^2\,(\Delta\phi/2\pi)$)
- Laboratory plasmas stabilized by applied ``vertical'' field B_Z, where $J_\phi \times B_Z$ is in -$\hat{\mathbf{R}}$ direction, force $F_V \sim \varepsilon^2\,\mathcal{A}\Delta\phi$
- Coronal loops have both ends (footpoints) tied in the photosphere, so only the upper part of the loop is unstable $\Rightarrow$ local force over $\Delta\phi$, acts on sin ϕ Fourier components
- Gravity is a radially inward force acting on the top of the loop, $F_g \sim -\rho g R\,\mathcal{A}\Delta\phi$. Magnitude $\rho g \sim \varepsilon p$ can balance radial expansion!

MHD normalization

Usual MHD normalization gives momentum equation

$$\hat{\mathbf{J}} \times \hat{\mathbf{B}} - \hat{\nabla}\hat{p} - \hat{\rho}\hat{G}\hat{\mathbf{h}} - \epsilon^2\hat{\rho}(\hat{\mathbf{v}}\cdot\hat{\nabla})\hat{\mathbf{v}} = \epsilon^2\hat{\rho}\frac{\partial\hat{\mathbf{v}}}{\partial\hat{t}} = 0.$$

⇒ Gravitational parameter $\hat{G}$=g a/v_A^2

Writing magnetic field as ($\perp$ is perpendicular to $\nabla\phi$)

$\mathbf{B} = \nabla_\perp\psi \times \nabla\phi + (1/R)\nabla_\perp F + R_o I\nabla\phi$ and $\mathbf{J} = \nabla\times\mathbf{B}$ gives

$$(R_oI/R^2)\left[-\nabla_\perp\tilde{I} + (1/R)\nabla_\perp(\partial\psi/\partial\phi)\times\hat{\boldsymbol{\phi}} + (1/R)\nabla_\perp(\partial F/\partial\phi)\right]$$
$$+(RJ_\phi/R^2)\left[\nabla_\perp\psi + (\partial F/\partial R)\hat{\mathbf{Z}} - (\partial F/\partial Z)\hat{\mathbf{R}})\right]$$
$$+\hat{\boldsymbol{\phi}}\,(1/R^2)\left[\nabla_\perp\tilde{I}\times\nabla_\perp\psi\cdot\hat{\boldsymbol{\phi}} - (1/R)\nabla_\perp(\partial F/\partial\phi)\times\nabla_\perp\psi\cdot\hat{\boldsymbol{\phi}}\right.$$
$$\left.+\nabla_\perp\tilde{I}\cdot\nabla_\perp F - (1/R)\nabla_\perp(\partial F/\partial\phi)\cdot\nabla_\perp F\right]$$
$$-\nabla p - \rho\hat{G}(\sin\phi\,\hat{\mathbf{R}} + \cos\phi\,\hat{\boldsymbol{\phi}}) - \epsilon^2\rho(\mathbf{v}\cdot\nabla)\mathbf{v} = 0$$

Elliptic structure – magnetic flux function

- Perpendicular momentum equation (to two orders in ϵ)

$$-\Delta^*\psi\,\nabla_\perp\psi = -R_o I(\nabla_\perp \tilde{I} - (1/R)\nabla_\perp(\partial\psi/\partial\phi)\times\hat{\boldsymbol{\phi}}) - R^2\nabla_\perp p - R^2\rho\hat{G}\sin\phi\,\hat{\mathbf{R}}. \tag{E1}$$

For smaller $\hat{G} = O(\epsilon^3)$, it reduces to the Grad-Shafranov equation

$$\Delta^*\psi = -(R_o^2/2)(dI^2(\psi)/d\psi) - R^2(dp(\psi)/d\psi). \tag{E2}$$

- A helical configuration requires a second relation, such as $\nabla\cdot\mathbf{J} = 0$. To lowest order in ϵ,

$$\begin{aligned}\left[(\mathbf{B}\cdot\nabla) \;+\; R_o\hat{G}\sin\phi\right]\nabla_\perp^2\psi_0 &= -2\nabla_\perp p\cdot\hat{\mathbf{Z}} \\ -\;\; (R_o\hat{G}/B)\nabla_\perp\rho\cdot\hat{\mathbf{Z}}\,\sin\phi &- (R_o\hat{G}/B^2)\nabla_\perp\rho\cdot\nabla_\perp\psi\,\cos\phi\end{aligned} \tag{E3}$$

At high beta, $\nabla_\perp p \sim \epsilon$, $(\mathbf{B}\cdot\nabla)$, and $\hat{G}\sim\epsilon^2$ give same order terms. (The high beta stellarator relation, where $\hat{G}=0$ and $\mathbf{B}$ supplies the nonaxisymmetry, is $(\mathbf{B}\cdot\nabla)(\nabla_\perp^2\psi_0) = -2\epsilon\nabla_\perp p_1\cdot\hat{\mathbf{Z}}$.)

- Solution requires specification of loop boundary surface $\psi_{\rm eff}^{\rm bdy}$.

Flux function $\psi_{\rm eff}$ constrains p, T, n

- Helical laboratory plasmas satisfy $\mathbf{J} \times \mathbf{B} = \nabla p$, so $\mathbf{B} \cdot \nabla p = 0$ and p is a magnetic flux function (field lines stay on same constant-p surface). The coronal loop has gravity, so

$$\mathbf{B} \cdot [\nabla p + \rho \nabla \Phi_g] = 0, \qquad \Phi_g \equiv \hat{G} R \sin\phi$$

  Pressure and temperature profiles of the form

$$p = P(\psi_{\rm eff}) \exp[-M_i \Phi_g / T], \qquad T = T(\psi_{\rm eff})$$

  for arbitrary functions $P(\psi_{\rm eff})$ and $T(\psi_{\rm eff})$, yields $\mathbf{B} \cdot \nabla \psi_{\rm eff} = 0$ and $\psi_{\rm eff}$ is a flux function To lowest order(s) in ϵ, $\psi_{\rm eff} = \psi$. (Other p, T forms are possible, but behave similarly.)

- $T = T(\psi_{\rm eff})$ is consistent with (1) Extreme UltraViolet T is observed to be constant over coronal part of many loops and (2) large parallel thermal conductivity in loop.

- p, $n \equiv p/2T$, and T can all be non-axisymmetric, due to the hydrostatic exponential factor and/or $\psi_{\rm eff}$.

Results: Gravitational loop solutions

- Gravity balances the radial expansion force in only three parameter ranges (for a ``flux rope'' coronal loop with dominant axisymmetric toroidal field $B_\phi=(R_o I/R)(1+\varepsilon\tilde{I})$).
  - High beta ($\beta\sim\varepsilon^1$) and $\hat{G}\sim\varepsilon^3$ --- high beta tokamak core plus non-axisym.
  - High beta ($\beta\sim\varepsilon^1$) and $\hat{G}\sim\varepsilon^2$ --- strong nonaxisymmetry
  - Low beta ($\beta\sim\varepsilon^2$) and $\hat{G}\sim\varepsilon^3$ --- axisymm tokamak core + non-axisymm p
  - $\hat{G}\sim\varepsilon^1$ and $\hat{G}=O(\varepsilon^4)$ and smaller are not possible
- The $\hat{G}$ force balances the lowest order sin ϕ component of ψ, at order ε^0 or ε^1 (ψ_{0s} or ψ_{1s}) as determined by p_{1s}or p_{2s}.
  - Elliptic solution for ψ_{eff} requires specification of the Fourier components of the plasma boundary surface. Axisymmetric and cos ϕ pieces are fixed by the two loop footpoints at $\phi=0$ and π, but $\hat{G}$ is needed to fix a stationary sin ϕ surface at the top of the loop.
  - Radial expansion force at the loop top is the same order as in a torus.
  - Minimum radial force is set by B_{pol} hoop force at local $F_H\sim\varepsilon^3$. Thus, gravitational loop solution with $\hat{G} < \varepsilon^3$ is not possible.

Good fit to observations

- Coronal loops in a solar active region
  - From studies of heating by Alfvén Wave fluctuations (2010-2015)
- Magnetic field line was fit to a chosen bright emission curve (AIA 171Å) using line-of-sight magnetograms and nonlinear force-free field (NLFF) model for **B**
  - HMI (on Solar Data Observatory) magnetograms measure B in the photosphere at $(700\ \mathrm{km})^2$ resolution (loop $a \approx 1000$ km)
  - NLFF model inserts and connects coronal loop field lines into a background potential field $\mathbf{J}\times\mathbf{B}=0$, $\mathbf{B}=\nabla\Phi$ (CMS code)
- Gravity gives good fit to observed warm and short hot loops
  - $\hat{G}$ increases with R_o, $\hat{G}$ scaling falls in predicted range for high beta
  - Short hot loops, shortest warm loops match $\hat{G}\sim\varepsilon^3$
  - Long warm loops match $\hat{G}\sim\varepsilon^2$; intermediate length loops fall in between

Observations

Table I. Active Region NOAA 11564, 7 Sept 2012

Loop	R_o (10^7m)	a/R_o	n_o (10^{15}m^{-3})	T_o (10^6K)	B_o (G)	v_A (10^6 m/s)	τ_A (s)	β_o (10^{-2})	$\hat{G}$ (10^{-4})	$\hat{G}/\epsilon^3$	$\hat{G}/\epsilon^2$	H_{LR}
H2	1.04	0.0247	28.50	4.88	213	2.75	3.77	2.12	0.093	0.62	0.015	14.1
H1	1.98	0.0157	18.17	5.36	144	2.33	8.49	3.25	0.16	4.06	0.064	8.12
F4	2.05	0.0311	2.72	2.48	34.0	1.42	14.4	4.05	0.87	2.88	0.090	3.63
F1	2.47	0.0184	2.58	2.65	68.0	2.92	8.47	1.03	0.15	2.37	0.044	3.21
F5	2.61	0.0207	2.52	2.64	48.0	2.08	12.5	2.00	0.34	3.84	0.080	3.04
F9	4.21	0.0133	2.17	2.84	44.7	2.09	20.1	2.14	0.35	-	0.20	2.56
F3	5.90	0.0130	1.39	2.75	24.0	1.40	42.0	4.61	1.07	-	0.64	1.40
F8	5.90	0.0143	1.11	1.95	19.6	1.28	46.0	3.91	1.41	-	0.69	0.99
F7	9.81	0.0115	1.06	1.97	11.0	0.74	133.	12.0	5.72	-	4.32	0.60
F2	10.3	0.0128	0.83	2.09	8.0	0.60	170.	18.8	9.88	-	6.05	0.61

H1,2: short hot loops ("r7" [MAT15]).
F1-5,7-9: warm loops [MAT14]. Loop F6 did not converge in the NLFF model.

- Typical coronal loop parameters at loop-top

$R_o = 1 - 10 \times 10^7$ m $v_A = 4 - 0.5 \times 10^6$ m/s

$\varepsilon = a/R_o \simeq 0.02$ $\tau_A = 4 - 170$ s

$B_o = 210 - 10$ G $\beta_o = 0.005 - 0.27$

$n_o = 10 - 1 \times 10^{15}$ m^{-3} $\hat{G} = 0.06 - 13. \times 10^{-4}$

$T_o = 5 - 1 \times 10^6$ K (10^6 K=86 eV) range: $\hat{G}/\varepsilon^3 \gtrsim 0.56$ to $\hat{G}/\varepsilon^2 \lesssim 6$

Table II. Active Region NOAA 11067, 5 May 2010

Loop	R_o (10^7m)	a/R_o	n_o (10^{15}m^{-3})	T_o (10^6K)	B_o (G)	v_A (10^6 m/s)	τ_A (s)	β_o (10^{-2})	$\hat{G}$ (10^{-4})	$\hat{G}/\epsilon^3$	$\hat{G}/\epsilon^2$	H_{LR}
F8	2.51	0.0258	3.86	2.96	33.4	1.172	21.4	7.11	1.30	7.55	0.195	3.54
F5	2.67	0.0261	3.38	2.86	28.6	1.073	24.9	8.19	1.67	9.34	0.244	3.21
F7	2.68	0.0312	2.96	2.44	20.1	0.810	33.2	12.4	3.52	11.6	0.363	2.73
F3	2.85	0.0248	3.53	2.81	28.0	1.027	27.8	8.79	1.84	12.1	0.299	3.96
F1	3.42	0.0240	2.84	2.57	21.0	0.859	39.8	11.5	3.05	-	0.530	2.26
F6	3.42	0.0290	2.43	2.30	14.2	0.630	54.2	19.1	6.86	-	0.816	2.02
F4	4.10	0.0271	2.04	2.09	11.3	0.547	75.0	23.1	10.21	-	1.390	1.53

Longest loops (4,6,1) are fit by $\hat{G}_2$, others fall between $\hat{G}_3$ and $\hat{G}_2$. Loops 2,9 did not converge in the NLFF model.

Table III. Active Region NOAA 11428, 7 March 2012

Loop	R_o (10^7m)	a/R_o	n_o (10^{15}m^{-3})	T_o (10^6K)	B_o (G)	v_A (10^6 m/s)	τ_A (s)	β_o (10^{-2})	$\hat{G}$ (10^{-4})	$\hat{G}/\epsilon^3$	$\hat{G}/\epsilon^2$	H_{LR}
F8	1.55	0.0219	4.42	2.38	121.9	3.996	3.9	0.491	0.0584	0.555	0.0122	4.61
F15	1.56	0.0218	4.44	2.35	121.2	3.964	3.9	0.493	0.0595	0.571	0.0125	4.53
F6	1.62	0.0214	4.17	2.28	116.1	3.918	4.1	0.490	0.0621	0.633	0.0136	4.22
F3	1.69	0.0214	4.40	2.31	106.9	3.513	4.8	0.617	0.0806	0.825	0.0176	4.09
F7	1.87	0.0232	3.54	2.62	74.2	2.717	6.9	1.17	0.162	1.30	0.0301	4.19
F1	1.90	0.0323	4.28	2.56	37.0	1.234	15.4	5.54	1.11	3.29	0.106	4.03
F2	1.96	0.0205	4.18	2.27	86.8	2.926	6.7	0.874	0.129	1.49	0.0306	3.25
F12	2.73	0.0191	3.41	2.05	51.5	1.924	14.2	1.83	0.387	5.59	0.107	2.25
F5	2.76	0.0206	3.74	2.71	43.4	1.548	17.8	3.73	0.651	7.47	0.154	2.95
F13	2.99	0.0215	3.14	2.40	33.8	1.316	22.7	4.57	1.021	10.2	0.220	2.41
F18	3.21	0.0181	3.12	1.92	41.6	1.623	19.8	2.40	0.605	10.2	0.185	1.80
F4*	2.66	0.0330	2.35	2.19	18.1	0.816	32.7	10.85	3.63	10.1	0.334	2.47
F19	5.65	0.0225	1.31	2.20	8.68	0.523	108.1	26.6	12.77	-	2.53	1.17

Loops"r2" from Table 1 in [MAT13]. Loops 9,10 not included. 11,14,16,17,20,21,22 did not converge in NLFF model.
*F4 ordered by B_o, not R_o.

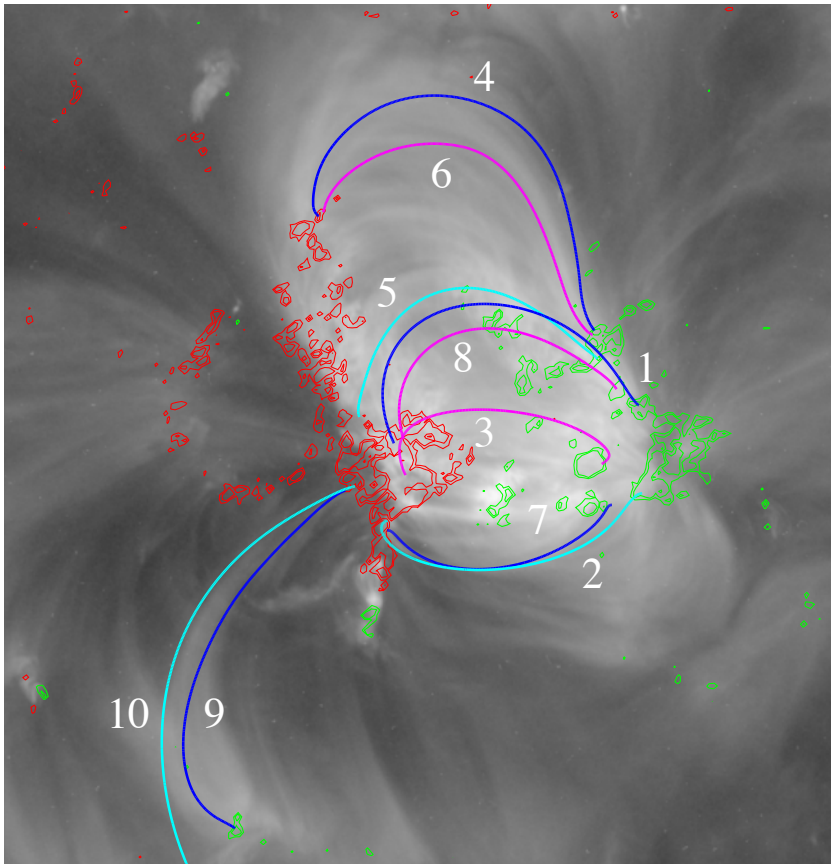

Active Region NOAA 11067, 5 May 2010
Table II

(Loops 2,9 do not converge in NLFF model.
Line 10 Is not a loop -- no emission curve.)

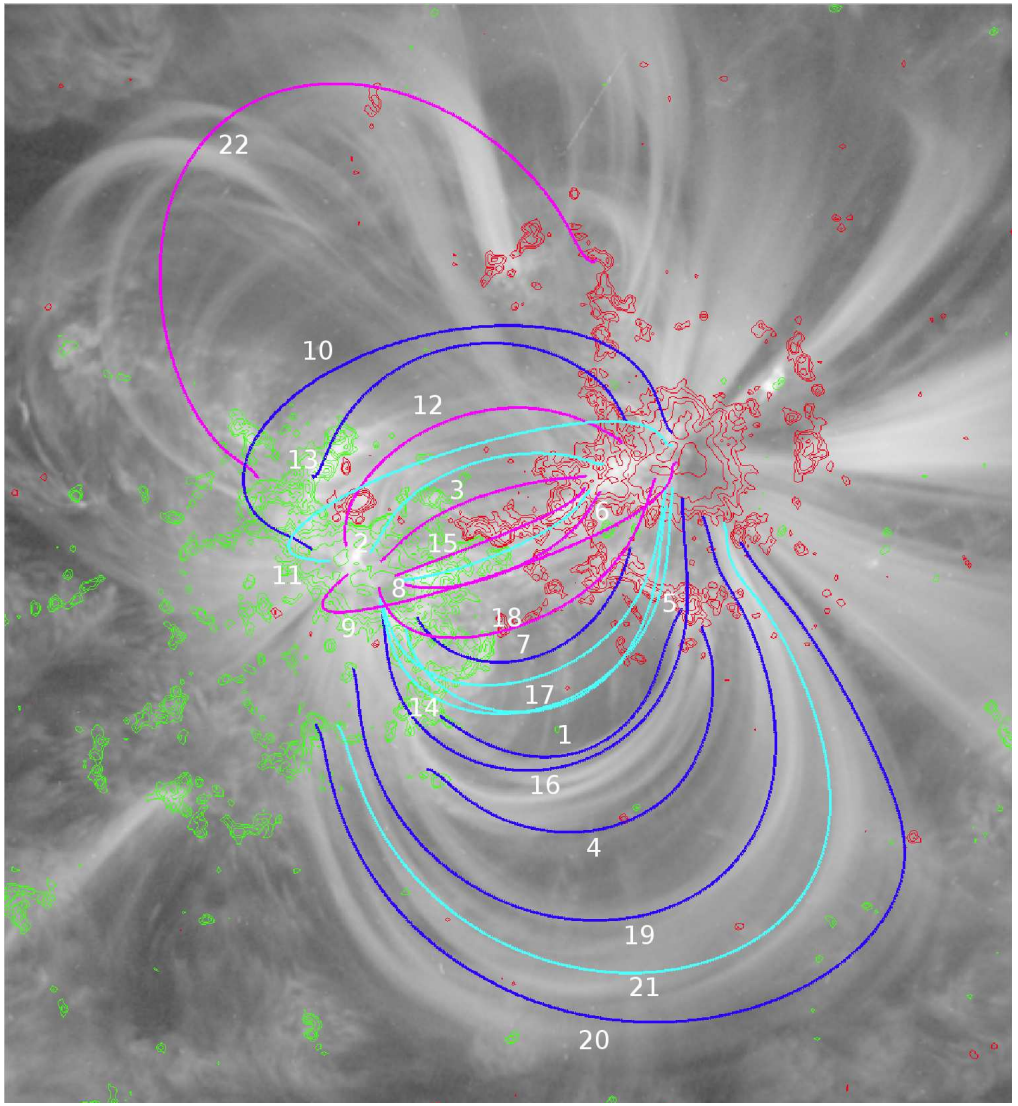

Active Region NOAA 11428, 7 March 2012, Table III

(Loops 11,14,16,17,20,21,22 do not converge in the NLFF model)

- Physical picture – loop should expand up to its characteristic height, where it reaches a quasi-steady state
  - An expanding loop at lower height has larger B and n at the loop top, so net $\hat{G}$ is smaller and cannot balance the radial expansion force
- Time scales are consistent with observed loop lifetimes
  - Lifetimes of 1000-5000 s for warm loops (shorter loops are longer lived) correspond to a force imbalance at order of ε^2 higher than the gravitational balance for shorter warm loops (ε^5 for $\hat{G}_3$ or timescale 250x longer,) or $\varepsilon^{1.2}$ higher for $\hat{G}_2$ loops (timescale x 109)
- Model is compatible with longer loops acting as seeds for coronal mass ejections (CMEs):
  - Beyond a certain height, loops will be metastable, because gravity begins to decrease with height as $g \sim (R_o + R_{sun})^{-2}$, where R_{sun} is the photosphere radius 69.55x 10^7 m.
  - Longer loops are more non-axisymmetric
  - CME loops grow large, $R_o \approx 1—10^+ R_{sun}$, appear strongly non-axisymmetric, grow by radial expansion where gravity is not important

Summary

- MHD steady states for coronal loops in solar active regions, described as non-axisymmetric magnetic flux ropes, are derived for the first time. The ``weak'' solar gravity is crucial, to stabilize the toroidal radial expansion force.
  - Gravitational parameter $\hat{G} = ga/v_A^2 \sim ga(n_o/B_o^2)$ at loop top
- Two analytical steady states exist at high beta $\beta \sim \varepsilon^1$, at $\hat{G} \sim \varepsilon^3$ and $\hat{G} \sim \varepsilon^2$ in terms of small inverse aspect ratio $\varepsilon = a/R_o \sim 0.02$
  - Pressure, temperature, cross-section are mostly free functions
  - Loop height and non-axisymmetry increase with $\hat{G}$
  - Relation/reduction to high beta tokamak and stellarator
- Good fit to observed warm/hot loops in active regions!
- Many implications for solar physics, including CMEs
  - Sun is complex - need more comparison to better observations

Summary -2-

- Numerical solutions are possible using nonlinear 3D fusion simulation codes
  - Easy to add gravity; loop footpoints harder but do-able
  - Steady state for longer $\hat{G}_2$ loops needs numerical solution (nonaxisymmetric)
  - Time-dependent studies of radial expansion and evolution, especially for longer loops
  - But, need more information on actual loops to constrain results
- Improve the NLFF magnetic model, widely used for analysis of solar magnetic loops (CMS code, 22,000 lines)

Remarks: edge simulations with M3D-C1, M3D

- A number of differences between codes exist in the treatment of the MHD equations and terms, Grad-Shafranov equilbrium, and unconfined field region (``resistive vacuum'')
- Linear growth rate comparison – find good scaling of test case in toroidal mode number n using M3D-C1 (since M3D has less efficient linear solution), then run M3D to compare. Baseline is old M3D solutions at low resolution (from NL 2010 case, should be recomputed)
- Initial comparisons used suggested M3DC1 parameters – poor results
- Difficult to determine the exact profiles used in code; documentation not up-to-date; code changing

EFIT reconstruction – plasma edge

- GEQDSK files for experimental reconstructions are not very accurate for the plasma edge (even 257x257)
- Flux $\psi(R,Z)$ is given on nx by nh rectangular grid
  - nx points over radius from inner to outer wall => grid spacing at plasma edge can be $\gtrsim$ edge ∇p or J_{BS} layer widths
  - Actual EFIT solution is more accurate; gives separatrix and outer wall
  - Confirmed by Lang Lao for DIII-D H-mode case
- Use EFIT magnetic axis, separatrix curve, and outer wall for most accurate GS equilibrium
  - Showed differences between separatrix and interpolated ψ for M3D a year or so ago at CEMM
  - Bootstrap J_{BS} most sensitive (?)

Differences in dissipation

- Viscosity – strong effect at high n-numbers
  - Artificial increase of viscosity well inside plasma edge – make sure to turn off
  - Real: diffusion term $(1/\rho)\nabla\cdot(\mu\nabla\mathbf{V})$ compared to $(\mu/\rho)\nabla^2\mathbf{V}$ with approximate diffusion coefficient μ/ρ =const
  - M3D edge effective viscosity significantly smaller than M3D-C1
- Resistivity outside plasma: neutrals, impurities
  - η > Spitzer value based on T_e, due to higher collisionality from neutrals, impurities (Z_{eff}). Is plasma Maxwellian?
    - Need to set plasma edge/SOL η-value independently of T, n
  - Also inside plasma near base of edge pedestal
- Thermal conductivity $n\kappa$ --- need to set κ independently of n in plasma edge (steep ∇n)

DIII-D 126006.03600 M3DC1 linear eigenspectrum

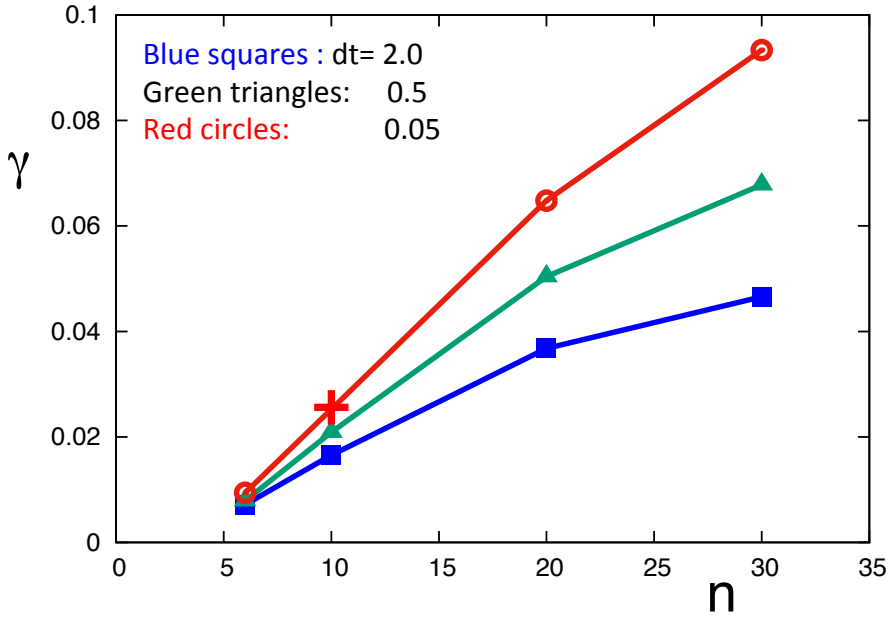

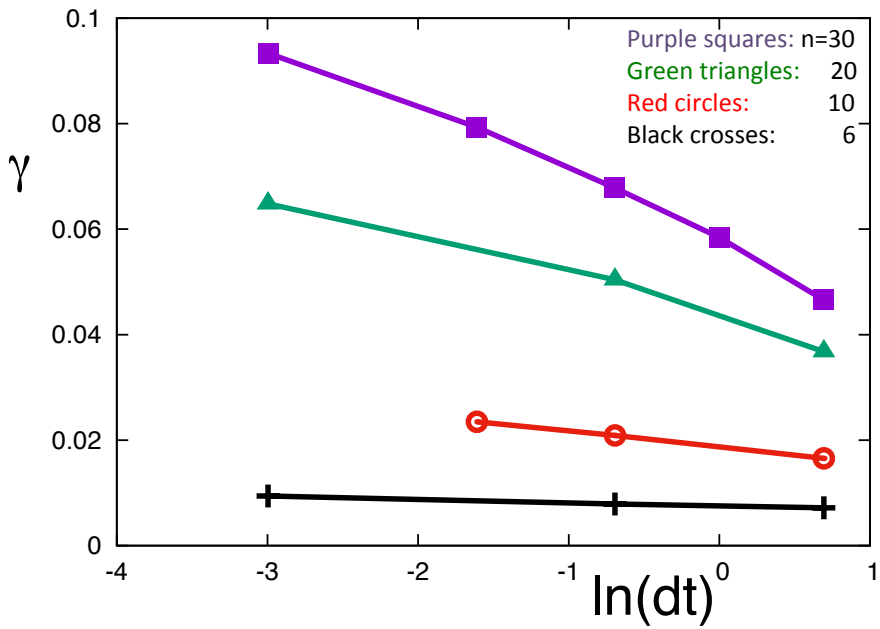

- Original time stepping parameters - Linear growth rate γ increases at smaller time step dt for (R,Z) mesh SJ2e. Converging, but numerical instability at very small dt, where growth rate begins to oscillate with increasing amplitude (dt=0.05 at n=10, 0.01 at n=30). Improved time-stepping parameters speed up convergence and removes most dt-dependence (dt=1.0 close to dt=0.05), but growth rates are similar/higher than maximum (small dt) values at orig time-step parameters here.
- Left: as function of toroidal mode number n
- Right: as function of ln(time step) (log 10 scale)

Resistive and viscous effects: n=30

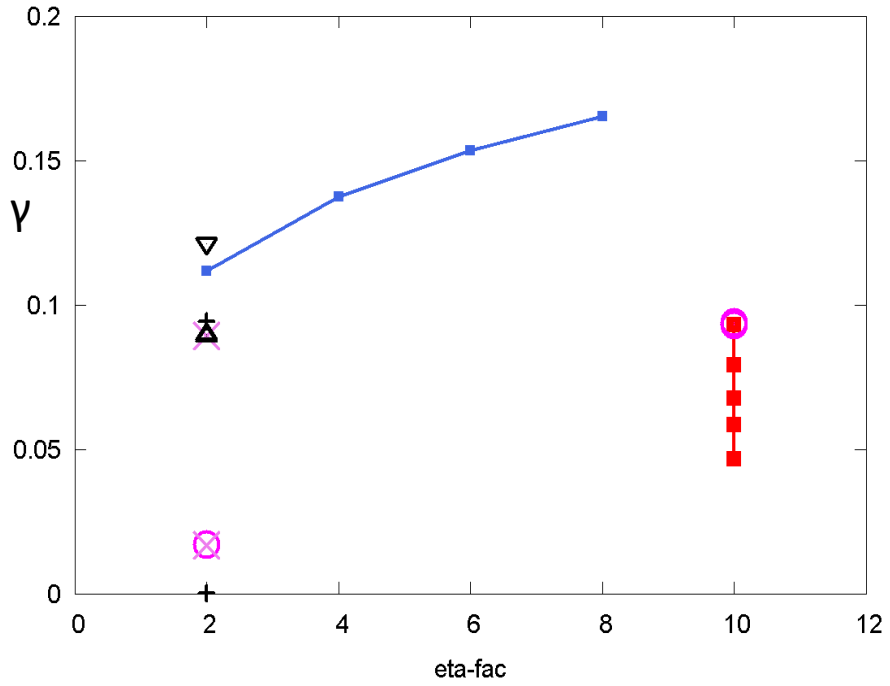

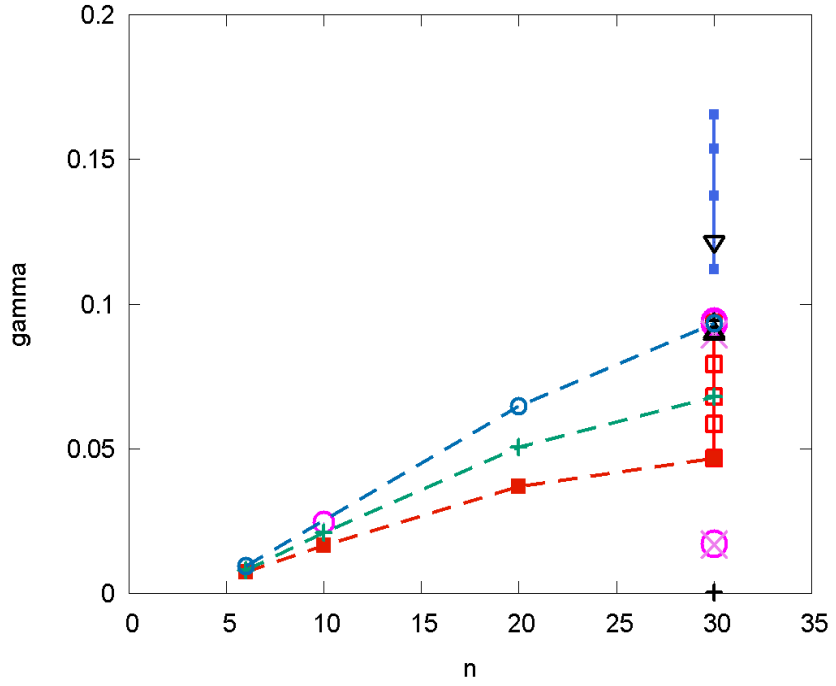

- Growth rates for n=30 harmonic (Z_{eff}=1). Left: vs eta. Right: compare to original.
- Resistivity factor eta_fac (multiplier of Spitzer resistivity): blue line/squares
  - SOL value depends on p_edge (input parameter),not independent of p(x)
- Ion (perpendicular) viscosity: triangles, circles, X's, crosses for different values and varying profiles.
  - Crosses show μ = 1.e-5 and 1.e-6 with uniform profile: almost stable -> huge γ
- Time step dt (red) at eta_fac=10 for the older time-stepping parameters
- Coarse grid => poorly converged results, but trends are correct

Summary

- Solar coronal loop as a MHD magnetic flux rope with gravity – based on modern observations, analysis
  - Analytical solution is robust
  - Very specific predictions for possible steady states fit observations surprisingly well
  - More comparison with observations needed before numerical solution (ongoing)
  - Many implications for solar physics and models
- For magnetic fusion – loop is an example of low-n nonaxisymmetric effects in a toroidal plasma
- Remarks on edge simulations